**Proceedings of 14th IOE Graduate Conference**
*Peer Reviewed*
Year: 2023 Month: December Volume: 14
ISSN: 2350-8914 (Online), 2350-8906 (Print)

# Study of Variation in Structural and Hydraulic Properties of Porous Concrete

Rabin Lamichhane [a], Gokarna Bahadur Motra [b], Thaman Bahadur Khadka [c]

[a, b, c] *Department of Civil Engineering, Pulchowk campus, IOE, Tribhuvan University, Nepal*
[a] 078msste013.rabin@pcampus.edu.np, [b] gmotra@ioe.edu.np, [c] thamankhadka@pcampus.edu.np

**Abstract**
Urbanization has led to a significant increase in impervious surfaces due to the conversion of natural lands, resulting in adverse environmental impacts like groundwater depletion. Porous concrete emerges as a potential sustainable solution to mitigate these effects by allowing rainwater percolation and groundwater recharge. This experimental study investigated the structural and hydraulic behavior of porous concrete under varying moisture conditions and porosity levels. Specimens in both cubical and cylindrical shapes were prepared, targeting porosities of 15%, 20%, and 25%. Compressive strength testing was conducted on specimens with a target porosity of 15% in three distinct states: oven-dried, air-dried and saturated. Additionally, density, porosity, and permeability measurements were recorded for specimens across all three target porosities. The results consistently revealed a decreasing trend in compressive strength as moisture content increased. Observed porosities surpassed all three target levels in a linear relationship, primarily due to inconsistencies in compaction levels resulting from the three-layer tamping method. The study further examined the influence of porosity on density and permeability. It was found that porosity exhibited a direct correlation with permeability, while showing an inverse correlation with density. Specifically, specimens with higher porosity demonstrated lower dry density but higher permeability. This research significantly contributes to the understanding of porous concrete behavior and performance under various moisture regimes and porosity levels.

**Keywords**
Porous Concrete, Urbanization, Moisture Condition, Compressive Strength, Density, Porosity, Permeability

## 1. Introduction

Urbanization has led to a significant increase in impermeable construction land, resulting in a reduction in natural permeable surfaces. In Kathmandu Valley, the conversion rate of permeable to impervious land was 11.78% in just a decade (2010 – 2020) [1]. Urbanization in the Himalayan Piedmont fan regions is presently occurring at a swift pace, resulting in the rapid depletion of groundwater and a significant drop in the water table [2]. Groundwater levels in Kathmandu Valley varied spatially from – 0.11 m to 11.5 m over two years (July 2017 – June 2019) [3]. Among many reasons, impermeable road construction materials such as bituminous and rigid concrete pavement is one of them. Application of such material significantly reduces the groundwater recharge and increases the rainwater runoff to the drainage body. As an alternative approach to reducing the negative impact of impermeable surfaces, porous concrete can act as a suitable means [4].

Porous concrete is a non-slumping, open-graded material comprising hydraulic cement, coarse aggregate, admixtures, and water, with connected pores ranging from 2 to 8 mm, void content typically between 15% to 35%, compressive strength of 2.8 MPa to 28 MPa, and a drainage rate of 81 to 730 L/Min/m², dependent on aggregate size and mixture density [5]. Porous concrete finds frequent application within permeable pavement systems, notably in roadways, sidewalks, driveways, parking lots, and various light-duty flatwork applications [6]. However, the rapid adoption of permeable pavement systems has resulted in significant challenges, including insufficient strength and durability mainly arising from the absence of standards for optimizing mixtures, designing pavements, and characterizing methods [7].

The primary aim of incorporating porous concrete into road pavement systems is to facilitate the infiltration of rainfall water, thereby recharging the groundwater system. Across different time spans, the porous concrete layer can experience diverse states, including complete dryness, partial dryness, or complete saturation. It becomes imperative for the porous concrete pavement to exhibit resilience against vehicular loads and other pertinent forces even in these varying scenarios. Consequently, ensuring the robust performance of porous concrete pavement across a range of moisture conditions becomes a crucial consideration. Considering the area, the variation in 90 days of compressive strength with compaction efforts was studied, and found that the sealed specimens showed a 5% increase in strength compared to saturated specimens and air-dry specimens exhibited a 13% higher strength than soaked specimens [8].

Additionally, assessing the permeability of porous concrete is essential to ensure sufficient water infiltration for groundwater recharge. The permeability of porous concrete is directly related to its porosity. Tests have demonstrated that achieving substantial percolation requires a minimum porosity of around 15% [9]. The relationship between permeability and porosity was examined, revealing an increase in permeability as porosity increased, though lacking a definite correlation [10].

The purpose of this study is therefore to determine the compressive strength of porous concrete at different moisture level conditions and also to evaluate the relationship of permeability and density with porosity.

## 2. Experiment

### 2.1 Materials

In this experimental investigation, Type I (Grade 43) Ordinary Portland cement (OPC) was selected as the primary binder The material collection and preparation procedures strictly adhered to the established guidelines set forth by ASTM codes. Only a singular group of aggregates was utilized in the study, with particle sizes conforming to those that passed through a 10 mm sieve and were retained on a 4.75 mm sieve. The common physical properties of the aggregates used are tabulated in Table 1 below.

**Table 1:** Properties of Aggregates

| Properties | Value |
|---|---|
| Aggregate Size | 10mm - 4.75mm |
| Specific Gravity | 2.64 |
| Bulk Density | 1542.57 kg/m³ |
| Water Absorption | 0.868% |
| Percentage Fines | 4.702% |
| Aggregate Impact Value | 35.40% |
| Aggregate Cruhing VAlue | 37.39% |
| Void Percentage | 41.50% |
| Cement Type | OPC |
| Cement Grade | Grade 43 |

### 2.2 Preparation of Specimens

The preparation of porous concrete specimens involved a comprehensive and sequential process with meticulous attention and precise execution to attain the desired porosity levels. Initially, a careful selection of materials was undertaken, followed by rigorous testing to evaluate their properties. Subsequently, the calculation of the mix design ratio determined the specific proportions of each constituent needed for the concrete blend. Precise measurements of the coarse aggregate were combined with cement to produce a dry mixture. The measured quantity of water was then added to this dry mix, resulting in the formation of a fresh concrete blend. This freshly prepared mixture was poured into molds in three distinct layers and conscientiously consolidated through tamping, adhering to the stringent standards outlined in ASTM C192 [11]. Subsequent to this, the molds were opened on the following day, and the samples were placed in a curing tank for a duration of 27 days to ensure optimal hydration and the progressive development of strength.

For a void ratio of 15%, a comprehensive set comprising 12 cube specimens and 12 cylindrical specimens was meticulously prepared. Within this sample pool, a subset of 9 specimens underwent compressive strength testing, with 3 specimens tested under each of the following conditions: oven-dried, air-dried, and fully saturated states, encompassing both cubes and cylinders. Additionally, a smaller subset of 3 cube specimens and 3 cylindrical specimens was exclusively prepared for each targeted porosity level of 20% and 25%, earmarked specifically for porosity and permeability testing.

Further, different studies have been conducted for the preparation and mix design of porous concrete for defined porosity. To achieve the desired porosity ($\phi_{\text{design}}$) in the porous concrete mixture, the minimum volume of paste required ($v_{\text{p-min}}$) can be calculated using Equation 1 [12]:

$$v_{\text{p-min}} = v_{\text{void-agg}} - \phi_{\text{design}} \tag{1}$$

It is important to note that the calculation of $v_{\text{p-min}}$ assumes that the mixture's aggregates are being compacted in a way that resembles the ASTM C 29 (DRUW) procedure [13]. Additionally, this calculation presumes that the paste component is comparatively incompressible. The mix design proportion for each sample is shown in Table 2.

**Table 2:** Mix Proportions for Different Void Percentages

| Sample | Mix Proportion (Cement:Aggregate) | w/c Ratio | Target Void Percentage |
|---|---|---|---|
| A, B | 1 : 4.16 | 0.4 | 15% |
| C | 1 : 5.13 | | 20% |
| D | 1 : 6.69 | | 25% |

### 2.3 Testing

The test methods used in this study are the study of:

1. Structural Property (Compressive strength)
2. Physical Property (Density) and Hydraulic Properties (Porosity and Permeability)

#### 2.3.1 Compressive Strength

The compressive strength tests were conducted on specimens under different conditions: oven-dried, air-dried, and fully saturated. After curing, the specimens were soaked for 24 hours, air-dried for 24 hours, or oven-dried for 24 hours as per the condition. The compressive strength values were recorded following ASTM C39 standard for all specimens [14].The testing was conducted using a Compression Testing Machine, as illustrated in Figures 1a and 1b below.

**(a)** Cubical Specimens **(b)** Cylindrical Specimens

**Figure 1:** CS Testing of Specimens

#### 2.3.2 Physical and Hydraulic Properties

The porosities of the specimens were determined from following equations[15]. All three types of porosities were calculated for each sample.

$$A_{\text{total}}(\%) = \left(1 - \frac{W_3 - W_1}{V_1 \times \rho_w}\right) \times 100 \tag{2}$$

$$A_{\text{open}}(\%) = \left(1 - \frac{W_2 - W_1}{V_1 \times \rho_w}\right) \times 100 \tag{3}$$

$$A_{\text{close}}(\%) = A_{\text{total}}(\%) - A_{\text{open}}(\%) \tag{4}$$

where $A_{\text{total}}$ represents the total porosity of the specimen and $A_{\text{open}}$ and $A_{\text{close}}$ are open and closed void ratios respectively. $W_1$ is the weight of specimen when it is submerged in water, $W_2$ is its weight in SSD condition, and $W_3$ is its weight when it has completely dried in an oven, $V_1$ is the volume of specimen and $\rho_w$ is the density of water.

A specially made falling head permeameter was used to determine the coefficient of permeability of specimen [10]. The specimens were dried and laterally confined with silicone and wall putty to stop water from seeping through the sides. For the cube specimens, an acrylic sheet was placed on top and coated with silicone. For the cylinder specimens, an HDPE pipe was positioned on top, fastened with a rubber gasket and a hose clamp. The prepared samples were then placed in the permeability test apparatus as shown in Figures 2a and 2b.

**(a)** Cubical Specimens **(b)** Cylindrical Specimens

**Figure 2:** Permeability Measurement Apparatus

Water was added to the tank until full, and the time taken for the water level to fall from fixed height of $h_1$ to $h_2$ was recorded for both cubes and cylinders. The coefficient of permeability (k) was calculated using Equation 5 [10] with fixed heights of 45 cm and 25 cm for cubes, and 65 cm and 45 cm for cylinders.

$$k = 2.303 \times \frac{al}{At} \times \log_{10}(\frac{h_1}{h_2}) \tag{5}$$

where k is the coefficient of permeability, a is the cross-section area of the standpipe, A is the cross-section area of the sample, l is the length of the sample, $h_1$ and $h_2$ are initial and final heads and t is the time for head fall.

Similarly, the dry and the SSD density were carried out by dividing oven-dried weight by the volume of the specimen and SSD weight by the volume of the specimen, respectively [16].

## 3. Results

### 3.1 Influence of moisture conditions on Compressive Strength

The compressive strength results are visually represented in Figure 3, depicting the performance of both cubical and cylindrical specimens across different moisture conditions. The observed compressive strength exhibited variations among the specimens under varying moisture levels. In the case of cubes, the highest compressive strength was recorded under oven-dried conditions, with an average value of 7.89 MPa. This was followed by air-dried cubes at 5.09 MPa and saturated cubes at 4.54 MPa. A similar trend emerged in cylinders, with oven-dried cylinders displaying an average compressive strength of 8.11 MPa, followed by air-dried cylinders at 5.66 MPa, and saturated cylinders at 4.90 MPa.

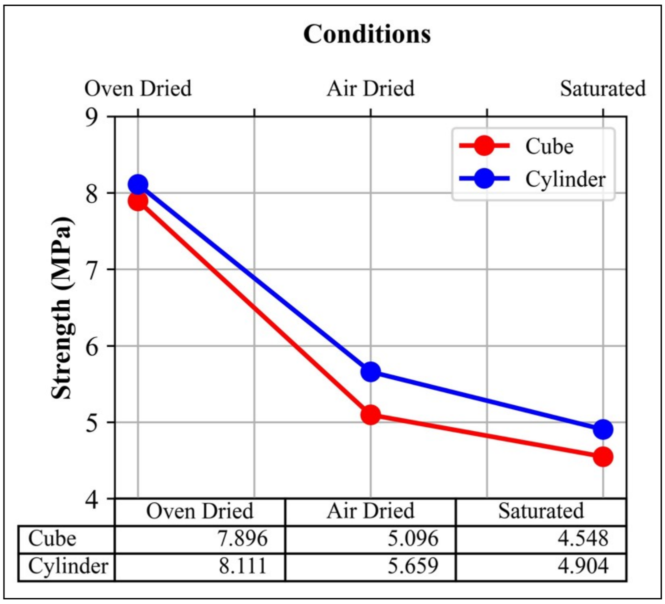


**Figure 3:** Compressive Strength of Cubes and Cylinders

In both cubical and cylinderical specimens, the compressive strength displayed a reduction of approximately 35.46% and 29.78% for air-dried conditions, and 42.40% and 39.54% for saturated conditions, respectively, when compared to the oven-dried condition. This consistent pattern of diminishing strength from oven-dried to saturated conditions underscores the material's susceptibility to the adverse impact of moisture on cohesion. Moisture intrusion weakens the interparticle bonds, resulting in reduced cohesion and adhesion within the concrete matrix. In addition to this the disruption of the cementitious matrix by water molecules, the potential for freeze-thaw cycles to induce cracking, and the possibility of chemical reactions between water and cementitious components, all of which collectively compromise the overall structural integrity of the material.

According to the analysis of the failure pattern, specimen failure occurs most frequently along the longitudinal sections that coincide with the grooves made when compacting concrete with a tamping rod. The observed failure pattern, as shown in Figures 4a and 4b, provides important information about how porous concrete behaves structurally. Clearly, the initial failure usually shows up at the top of the specimens. The distribution of compaction energy during the specimen preparation process, where the top layer receives comparatively less compaction energy compared to the underlying layers, can be attributed to this observed tendency.

**(a)** Cubical Specimens **(b)** Cylindrical Specimens

**Figure 4:** Failure Patterns

## 3.2 Variation of observed porosity with target porosity

The investigation of porosity in the specimens revealed discrepancies between the target and observed porosity values for both cylindrical and cubical specimens as shown in Figure 5.

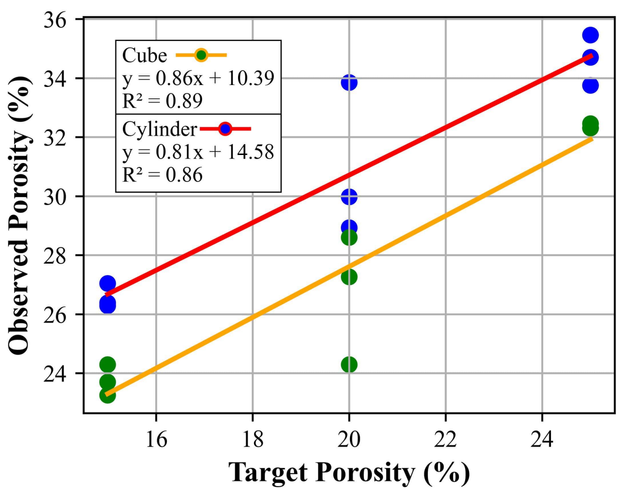


**Figure 5:** Observed Porosity versus Target Porosity

For the cylinders, the intended target porosity of 15% corresponded to an observed range of 26.28% to 27.04%. Similarly, the intended 20% target porosity exhibited an observed range spanning from 28.93% to 33.85%. Meanwhile, the 25% target porosity resulted in an observed range of 33.75% to 35.45%. The slope value of 0.81 indicates that, on average, for every 1% increase in the target porosity, the observed porosity tends to increase by approximately 0.81%.

Comparable trends were observed for the cubes, with the intended 15% target porosity translating to an observed range of 23.25% to 24.29%. Likewise, the intended 20% target porosity yielded an observed range ranging from 24.29% to 28.6%, while the 25% target porosity exhibited an observed range of 32.31% to 32.46%. On average, each 1% rise in the target porosity corresponds to an approximate 0.86% increase in the observed porosity.

These observed porosity values appear to increase in a linear fashion as the target porosity increases. Specifically, the cylinder specimens exhibited higher porosity levels compared to the cubes. This discrepancy can be attributed to the geometric differences between the two shapes, wherein the larger surface area of cylinders and the curved edges contributed to uneven compaction and, consequently, increased porosity.

Notably, the target porosity consistently exhibited lower values than the observed porosity. The observed differences primarily stem from the utilization of tamping as the compaction procedure during sample preparation, which led to variations in the applied compaction effort.

## 3.3 Influence of Porosity on Physical and Hydraulic Properties

### 3.3.1 Density

Figure 6 depict the correlation between the porosity and density of porous concrete for cylinders and cubes. The data clearly reveals that porosity exerts a direct influence on the density of porous concrete.

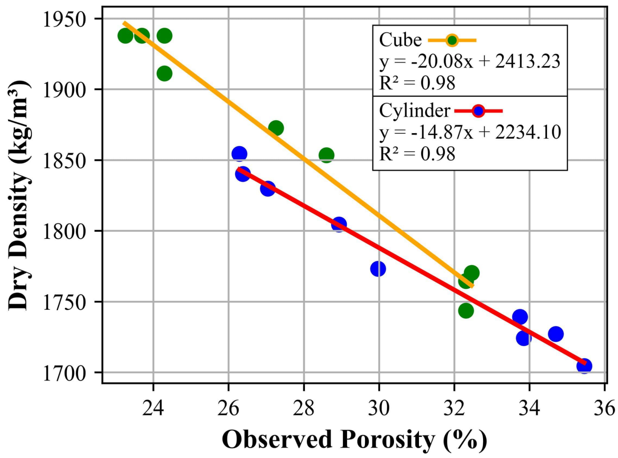


**Figure 6:** Dry Density versus Observed Porosity

The cylinders display porosity values ranging between 26.28% and 35.45%. Similarly, the dry density values exhibit variation from 1704.39 $kg/m^3$ to 1854.36 $kg/m^3$. A 1% increase in observed porosity correlates with a 14.87 $kg/m^3$ reduction in dry density, showing a strong inverse linear relationship with a very high R-squared value of 0.98.

Likewise, in the case of the cubes, observed porosity values range from 23.25% to 32.46%. Similarly, density values show variability spanning 1937.78 $kg/m^3$ to 1770.37 $kg/m^3$. As the observed porosity increases by 1%, the dry density decreases by a substantial 20.08 $kg/m^3$, highlighting an exceptionally robust and nearly linear inverse correlation with a very high R-squared value of 0.98.

Both configurations consistently demonstrate a pattern in which higher porosity aligns with lower dry density, illustrating an inverse correlation between porosity and density. This decline in density can primarily be attributed to the existence of larger voids and an augmented prevalence of voids within the porous concrete.

#### 3.3.2 Permeability

Figure 7 illustrate the correlation between the porosity and permeability of porous concrete for cylinders and cubes.

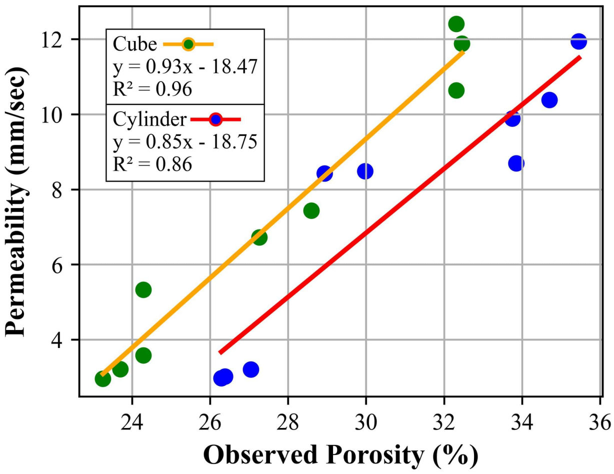


**Figure 7:** Permeability versus Observed Porosity

The data distinctly demonstrates that porosity significantly influences the permeability of porous concrete, unveiling a clearly discernible linear relationship. For the cylinders, the observed porosity values range between 26.28% and 35.45%, corresponding to permeability values spanning 2.97 mm/sec to 11.94 mm/sec. With a 1% increase in observed porosity, permeability increases by 0.85 mm/sec, reflecting nearly linear direct relationship supported by a R-squared value of 0.86.

Likewise, the porosity values observed in the cubes range from approximately 23.25% to 32.46%, corresponding to permeability values, ranging from 2.95 mm/sec to 11.88 mm/sec. An increase of 1% in observed porosity corresponds to a 0.93 mm/sec rise in permeability, emphasizing a strong, nearly linear, and directly proportional relationship with a high R-squared value of 0.96.

More precisely, with the rise in porosity of porous concrete, there is a corresponding increase in its permeability. This indicates a direct correlation between permeability and porosity. This phenomenon can be explained by noting the heightened presence of open voids within the porous structure as porosity increases. As a result, this expanded void space provides a larger surface area for water to permeate through the material.

## 4. Conclusion

From the results obtained, the following conclusions may be drawn:

1. The compressive strength of both cubical and cylindrical specimens consistently decreased with increasing moisture content, displaying the highest strength under Oven Dried conditions, followed by Air Dried and Saturated conditions, highlighting moisture's adverse impact on cohesion within the concrete matrix.
2. The observed porosity values were consistently higher than target porosity values due to discrepancies in compaction effort and sample preparation methods.
3. Increasing porosity in porous concrete is strongly correlated with reduced density due to the presence of larger voids.
4. Porosity directly impacts the permeability of porous concrete, showing a linear correlation. Higher porosity leads to increased permeability due to the presence of more open voids, offering a larger surface area for water to infiltrate.

## Acknowledgments

The authors wish to express their gratitude and sincere appreciation to Kathmandu Valley Water Supply Management Board for providing fellowship to the first author of the article through Centre for Water Resources Studies, Institute of Engineering, Tribhuvan University (CWRS, IOE, TU). The authors are also thankful to the staff of Material Testing Laboratory, Faculty of Civil Engineering both at Pulchowk Campus and Thapathali Campus for the facilities and support for experimental works.

## References

[1] Gyan Shrestha, Birendra M. Shakya, Madan B. Shrestha, and Uttam R. Khadka. Water infiltration rate in the kathmandu valley of nepal amidst present urbanization and land-use change. *H2Open Journal*, 6(1):1–14, 2023.

[2] Deepak K. Sahadevan and Ashok K. Pandey. Groundwater over-exploitation driven ground subsidence in the himalayan piedmont zone: Implication for aquifer health due to urbanization. *Journal of Hydrology*, 617:129085, 2023.

[3] Roshan Prajapati, Sangam Upadhyay, Rabindra Talchabhadel, Bibek Raj Thapa, Bivek Ertis, Pranay Silwal, and Jeffrey C. Davids. Investigating the nexus of groundwater levels, rainfall and land-use in the kathmandu valley, nepal. *Groundwater for Sustainable Development*, 14:100584, 2021.

[4] Rishi Gupta. Monitoring in situ performance of pervious concrete in british columbia—a pilot study. *Case Studies in Construction Materials*, 1:1–9, 2014.

[5] ACI Committee 522. Aci 522r-10: Report on pervious concrete. Technical documents, American Concrete Institute, 2010.

[6] Amminudin Ab Latif, Ramadhansyah Putrajaya, and Doh Shu Ing. A review of porous concrete pavement: Compressive strength and clogging investigation. *Journal of Advanced Research in Applied Sciences and Engineering Technology*, 29(3):128–138, 2023.

[7] Obada AlShareedah and Somayeh Nassiri. Pervious concrete mixture optimization, physical, and mechanical properties and pavement design: A review. *Journal of Cleaner Production*, 288:125095, 2021.

[8] Nader Ghafoori and Sujit Dutta. Laboratory investigation of compacted no-fines concrete for paving materials.

*Journal of Materials in Civil Engineering*, 7(3):183–191, 1995.

[9] Richard C Meininger. No-fines pervious concrete for paving. *Concrete International*, 10(8):20–27, 1988.

[10] Jan Olek, W Jason Weiss, Narayanan Neithalath, Adam Marolf, Eric Sell, and William Thornton. Development of quiet and durable porous portland cement concrete paving materials. Technical report, Purdue University, 2003.

[11] ASTM International. Standard practice for making and curing concrete test specimens in the laboratory. Standard, ASTM International, West Conshohocken, PA, 1998.

[12] Omkar Deo and Narayanan Neithalath. Compressive response of pervious concretes proportioned for desired porosities. *Construction and Building Materials*, 25(11):4181–4189, 2011.

[13] ASTM International. Standard test method for bulk density ("unit weight") and voids in aggregate. Standard, ASTM International, West Conshohocken, PA, 2017.

[14] ASTM International. Standard test method for compressive strength of cylindrical concrete specimens. Standard, ASTM International, West Conshohocken, PA, 1999.

[15] Dae Sik Seo. *An Experimental Study on Sound Absorption Properties of Multifunctional Porous Concrete for Building Materials*. PhD thesis, Chungnam National University, 2006.

[16] Narayanan Neithalath, Jason Weiss, and Jan Olek. Characterizing enhanced porosity concrete using electrical impedance to predict acoustic and hydraulic performance. *Cement and Concrete Research*, 36(11):2074–2085, 2006.